

## INFLUENCE OF MACHINING TECHNOLOGIES ON VALUES OF RESIDUAL STRESSES OF OXIDE CUTTING CERAMICS

JAKUB NĚMEČEK\*, KAMIL KOLAŘÍK, JIŘÍ ČAPEK, NIKOLAJ GANEV

*Department of Solid State Engineering, Faculty of Nuclear Science and Physical Engineering, Czech Technical University in Prague*

\* corresponding author: [j.nemecek91@gmail.com](mailto:j.nemecek91@gmail.com)

**ABSTRACT.** Currently, the intensive development of engineering ceramic and effort to replace sintered carbides as cutting materials are in progress. With the development of the sintering technology it is now possible to produce compact ceramic cutting samples with very good mechanical properties. The advantage of these materials is their easy accessibility and low purchase price. In this work, the influence of the finishing machine technology on the values of surface residual stresses of cutting ceramic samples  $\text{Al}_2\text{O}_3+\text{TiC}$  were studying. The samples were supplied by Moscow State University of Technology STANKIN. Measurements made in the X-ray diffraction laboratory at the Department of solid state engineering were performed for both the phases. The influence of the parameters of machining to residual stresses was studied and the resulting values were compared with each other.

**KEYWORDS:** Cutting ceramic; Machining technology; X-Ray diffraction; Residual stresses.

### 1. INTRODUCTION

Ceramic tools have been used since the Stone Age, when sandstone containing large amounts of silica blades was used, for example for the sharpening of knives, razor blades or other tools. This material was used henceforward as abrasive wheels during the ages of cutting weapons for sharpening of swords, knives and other blades. Only recently these grinding tools have been replaced by other modern materials for example by SiC or diamond.

At the beginning of the 20th century, the first use of  $\text{Al}_2\text{O}_3$  ceramics as a cutting tool occurred. Over the years, its development had moved to a level at which we were able to replace, for example, sintered carbides using those ceramic materials. This effort has been caused by the mechanical properties of aluminium oxide and the easy availability of the starting materials [1, 2].

The aim of this paper is to study the real structure of  $\text{Al}_2\text{O}_3+\text{TiC}$  oxide cutting ceramic. The microstrains and a size of crystallites was measured and influence of machining technologies on the macroscopic residual stresses was studied.

#### 1.1. PREPARATION OF SAMPLES

The starting materials and their properties have been known for a long time. The problem was how to make compact samples with the desired mechanical properties and dimensions. The current production process consists of three parts: first, grinding the starting material to a powder with grain size of the order of 100 nm, second, sintering the powders into a compact form and third, the surface treatment of the samples to the desired dimensions.

An important technological aspect of the properties of cutting ceramics is the grain size of the starting pow-

ders. If the individual grain size is approximately the same (if they have ideal spherical shape), the uniform distribution and the pore size are gained more easily during forming and thereby for uniform compaction throughout the volume and easier reorganization of the particles during sintering. Preference is also to achieve the smallest grain size of the sample, because it leads to faster material transport [3].

The sintering process is very similar to that used for sintered carbides. The powder is pressed below the melting point into a compact body, see Figure 1. But the main difference is the absence of a binder which during sintering formed a liquid phase, because it would cause degradation of mechanical properties. Today, ceramic is most commonly sintered into rods of cross section of finite samples and then cut to the desired dimensions. Individual plates are then variously surface treated and shaped [4].

### 2. X-RAY DIFFRACTION ANALYSIS OF MACROSCOPIC RESIDUAL STRESSES

In cooperation with the Moscow State Technological University STANKIN that provides manufacturing technology, the influence of machining technologies on the value of residual stresses in samples of  $\text{Al}_2\text{O}_3+\text{TiC}$  oxide cutting ceramics were investigated in X-ray diffraction laboratory of the Department of Solid State Engineering of FNSPE CTU in Prague. All experimental errors were around 10 % of absolute value of measurement.

#### 2.1. GRINDING BY DIAMOND DISC

After sintering, all samples were ground using a diamond wheel. An effect of displacement of the workpiece on the lift at constant cutting speed, feed rate



FIGURE 1. Scheme of creation technology of cutting ceramic sample: refinement powders (wet grinding), evaporation, pressing, sintering [5].

Sample	Fd, displacement on the lift [mm/displ.]	ap, depth of cut [mm]
1	0.5	0.04
2	1.0	0.04
3	1.5	0.04

TABLE 1. Parameters of grinding by diamond disc.

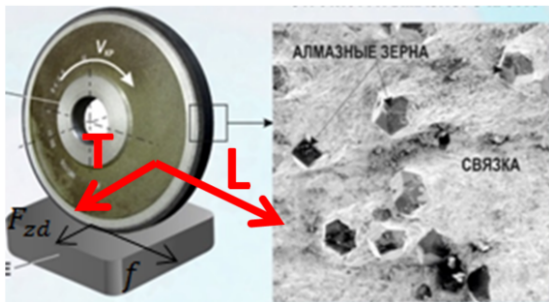


FIGURE 2. Scheme of grinding by diamond disc [5].

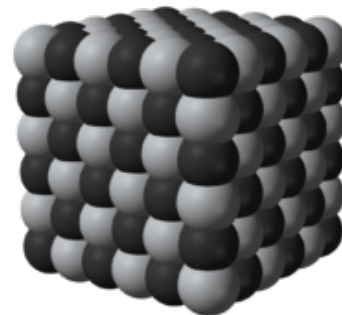
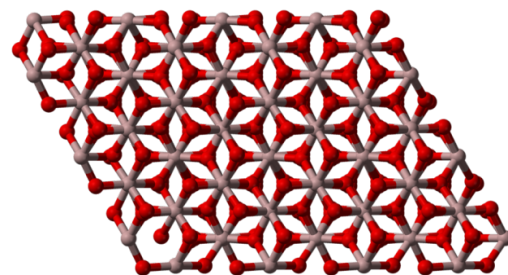


FIGURE 3. Structure of Al<sub>2</sub>O<sub>3</sub> (up) and TiC (down).

of the workpiece in the cutting direction and depth of cut was observed. Grinding parameters are given in Table 1, where cutting speed  $V_c = 30$  m/s and feed rate  $f = 12$  m/min.

Values of residual stresses were determined in two orthogonal directions L (direction of the grinding wheel) and T (direction of displacement on the lift). Because of unidirectional grinding anisotropy of values was observed in both directions. Different values are due to the different structure of Al<sub>2</sub>O<sub>3</sub> (trigonal) and TiC (cubic) and the different number of slip planes (see Table 2).

## 2.2. THERMAL ANNEALING OF THE SAMPLES AFTER GRINDING BY DIAMOND DISC

Next samples were ground by diamond disc with the same machining parameters and then thermally an-

nealed at 800 °C. It is evident from Table 3 that the values of the macroscopic residual stresses decreased considerably. In contrast, the value of microstrains and grain size given by the parameter FWHM remained almost unchanged.

## 2.3. AIR ABRASIVE MACHINING

In this method of machining, air of high pressure with added cutting microparticles is jetted on a rotating sample. The effect of air pressure changes on the residual stress in the sample was studied (Table 4) with constant time of blasting  $T = 60$  s and rotates per minute  $RPM = 50$ .

The obtained values (Table 5) show that when a pressure increases from 2 to 2.5 bars a decrease of compressive residual stresses (stress relaxation) is ob-

Al <sub>2</sub> O <sub>3</sub>				TiC			
L direction RS MnK $\alpha$ (0210)				L direction RS CrK $\alpha$ (311)			
Sample	$\sigma_N$ [MPa]	$\sigma_S$ [MPa]	FWHM [2 $\Theta$ ]	Sample	$\sigma_N$ [MPa]	$\sigma_S$ [MPa]	FWHM [2 $\Theta$ ]
1	-216	33	0.787	1	-518	77	0.759
2	-182	39	0.693	2	-536	77	0.741
3	-165	37	0.859	3	-530	74	0.708
T direction RS MnK $\alpha$ (0210)				T direction RS CrK $\alpha$ (311)			
Sample	$\sigma_N$ [MPa]	$\sigma_S$ [MPa]	FWHM [2 $\Theta$ ]	Sample	$\sigma_N$ [MPa]	$\sigma_S$ [MPa]	FWHM [2 $\Theta$ ]
1	-436	36	0.804	1	-776	67	0.668
2	-470	30	0.709	2	-805	93	0.759
3	-580	37	0.772	3	-938	89	0.679

TABLE 2. The values of normal ( $\sigma_N$ ) and shear ( $\sigma_S$ ) residual stresses after grinding by a diamond disc.

Al <sub>2</sub> O <sub>3</sub>				TiC			
L direction RS MnK $\alpha$ (0210)				L direction RS CrK $\alpha$ (311)			
Sample	$\sigma_N$ [MPa]	$\sigma_S$ [MPa]	FWHM [2 $\Theta$ ]	Sample	$\sigma_N$ [MPa]	$\sigma_S$ [MPa]	FWHM [2 $\Theta$ ]
12	-185	19	0.666	12	-516	91	0.965
13	-203	16	0.888	13	-290	40	0.609
14	-199	30	0.889	14	-289	112	0.847
T direction RS MnK $\alpha$ (0210)				T direction RS CrK $\alpha$ (311)			
Sample	$\sigma_N$ [MPa]	$\sigma_S$ [MPa]	FWHM [2 $\Theta$ ]	Sample	$\sigma_N$ [MPa]	$\sigma_S$ [MPa]	FWHM [2 $\Theta$ ]
12	-303	20	0.781	12	-599	71	0.782
13	-359	6	0.802	13	-474	57	0.613
14	-342	27	0.769	14	-473	104	0.908

TABLE 3. The values of normal ( $\sigma_N$ ) and shear ( $\sigma_S$ ) residual stresses after thermal annealing.

Sample	P, air pressure [MPa]
4	1.5
5	2.0
6	2.5

TABLE 4. Parameters of air abrasive machining.

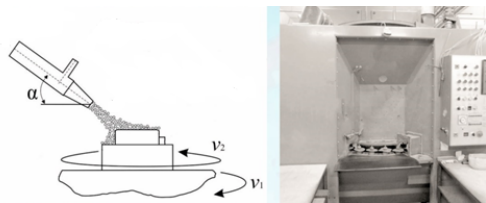


FIGURE 4. Scheme of air abrasive machining and a picture of machining chamber [5].

served. It is probably a result of overcoming the yield strength of the material. Perhaps machining process with higher pressure values influences deeper sub-surface layers of material. The energy required for

crack propagation is therefore higher for these seemingly lower pressure residual stresses. To confirm this assertion, a depth-profile analysis of residual stresses by sequential force-free etching of surface layers is needed.

Rotational movement of the specimen during the machining leads to an isotropic stress distribution i.e., the values in both the directions L and T are similar.

#### 2.4. WATER JET MACHINING

Water Jet Machining (WJM) is based on the same principle as air abrasive machining, when a focused beams of water is jetted out by varying the pressure on the rotating sample (see Figure 6 and Table 6). Other parameters: time of blasting  $T = 60$  s, distance of samples  $L = 2$  mm, number of nozzles  $N = 50$ .

It is evident, that for applied values of pressure jetting the yield strength value have not been overcome. The values of residual compressive residual stresses increase steadily with increasing pressure in contrast to the samples after air abrasive machining. Due to the rotating of the samples an isotropic residual stress distribution is achieved again (see Table 7).

Al <sub>2</sub> O <sub>3</sub>				TiC			
L direction RS MnKα (0210)				L direction RS CrKα (311)			
Sample	$\sigma_N$ [MPa]	$\sigma_S$ [MPa]	FWHM [2θ]	Sample	$\sigma_N$ [MPa]	$\sigma_S$ [MPa]	FWHM [2θ]
4	-352	34	0.787	4	-799	117	0.965
5	-367	45	0.694	5	-928	111	0.609
6	-242	32	0.827	6	-278	83	0.847
T direction RS MnKα (0210)				T direction RS CrKα (311)			
Sample	$\sigma_N$ [MPa]	$\sigma_S$ [MPa]	FWHM [2θ]	Sample	$\sigma_N$ [MPa]	$\sigma_S$ [MPa]	FWHM [2θ]
4	-295	42	0.781	4	-737	119	0.641
5	-389	44	0.802	5	-899	123	0.890
6	-284	36	0.769	6	-283	69	0.611

TABLE 5. The values of normal ( $\sigma_N$ ) and shear ( $\sigma_S$ ) residual stresses after air abrasive machining.

Sample	P, Pressure [MPa]
7	1.5
8	2.0
9	2.5

TABLE 6. Parameters of Water Jet Machining.

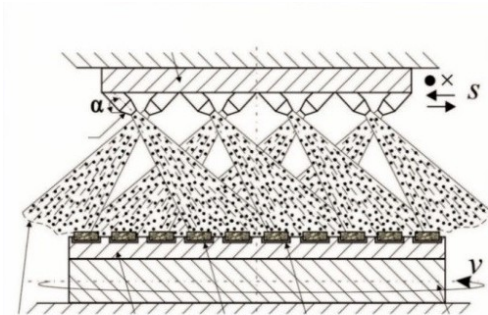


FIGURE 5. Scheme of Water Jet Machining.

### 2.5. LASER SHOCK PEENING

During machining by laser the samples are heated and it results in stress relaxation. Increased power (see Table 9) will lead to higher temperatures, and thus to higher stress relaxation. Furthermore, it is possible to observe the influence of the laying of individual spots (overlapping) on the anisotropy of distribution of residual stresses.

### 2.6. STRESS TESTS — THE EFFECT OF FRICTION

After grinding of samples by diamond disc their surface was loaded by rotating steel disk at different time intervals. The influence of time of friction on values of residual stresses was investigated (see table 10).

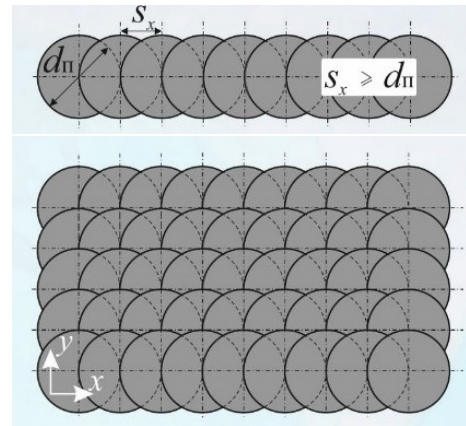


FIGURE 6. Scheme of linear and surface laying of spots for Laser shock Peening [5].

## 3. MICROSTRAINS AND CRYSTALLITE SIZE

Simultaneously with the measurement of the macroscopic residual stresses, determination of crystallite size and microstrains was provided using the Rietveld analysis. All results are demonstrated in [6].

From the measured values is evident that crystallite size after thermal annealing and after laser machining increased, which is probably due to recrystallization during these treatments. A decrease of microstrains is observed after air abrasive machining when the yield point was overcome and the grain sizes increased. After stress tests by steel disc the largest crystallite size Al<sub>2</sub>O<sub>3</sub> are observed, that could be again due to thermal relaxation and recrystallization of the surface.

## 4. CONCLUSIONS

Values of residual stresses of cutting ceramics Al<sub>2</sub>O<sub>3</sub>+TiC were analysed in two perpendicular directions. The influence of machining technologies to residual stresses was studied in both the phases.

Anisotropy and different values for the two phases during grinding by diamond disc were obtained, and

Al <sub>2</sub> O <sub>3</sub>				TiC			
L direction RS MnK $\alpha$ (0210)				L direction RS CrK $\alpha$ (311)			
Sample	$\sigma_N$ [MPa]	$\sigma_S$ [MPa]	FWHM [2 $\Theta$ ]	Sample	$\sigma_N$ [MPa]	$\sigma_S$ [MPa]	FWHM [2 $\Theta$ ]
7	-99	38	0.712	7	-406	118	0.644
8	-149	42	0.733	8	-363	74	0.691
9	-255	47	0.732	9	-568	118	0.765
T direction RS MnK $\alpha$ (0210)				T direction RS CrK $\alpha$ (311)			
Sample	$\sigma_N$ [MPa]	$\sigma_S$ [MPa]	FWHM [2 $\Theta$ ]	Sample	$\sigma_N$ [MPa]	$\sigma_S$ [MPa]	FWHM [2 $\Theta$ ]
7	-85	43	0.790	7	-374	116	0.644
8	-166	50	0.752	8	-364	88	0.689
9	-238	45	0.668	9	-484	108	0.669

TABLE 7. The values of normal ( $\sigma_N$ ) and shear ( $\sigma_S$ ) residual stresses after Water Jet Machining.

Al <sub>2</sub> O <sub>3</sub>				TiC			
L direction RS MnK $\alpha$ (0210)				L direction RS CrK $\alpha$ (311)			
Sample	$\sigma_N$ [MPa]	$\sigma_S$ [MPa]	FWHM [2 $\Theta$ ]	Sample	$\sigma_N$ [MPa]	$\sigma_S$ [MPa]	FWHM [2 $\Theta$ ]
10.1	-53	31	0.731	10.1	-318	111	0.594
10.2	31	31	0.717	10.2	-259	96	0.657
10.3	-29	23	0.757	10.3	-200	106	0.637
10.4	-62	17	0.751	10.4	-220	95	0.568
T direction RS MnK $\alpha$ (0210)				T direction RS CrK $\alpha$ (311)			
Sample	$\sigma_N$ [MPa]	$\sigma_S$ [MPa]	FWHM [2 $\Theta$ ]	Sample	$\sigma_N$ [MPa]	$\sigma_S$ [MPa]	FWHM [2 $\Theta$ ]
10.1	-155	9	0.856	10.1	-509	148	0.619
10.2	-125	9	0.868	10.2	-448	135	0.545
10.3	-71	42	0.737	10.3	-367	135	0.543
10.4	-48	39	0.704	10.4	-288	123	0.618

TABLE 8. The values of normal ( $\sigma_N$ ) and shear ( $\sigma_S$ ) residual stresses after Laser Shock Peening.

Sample	P, Power [W]	Sample	T, Time of loading [s]
10.1	2	11.1	2
10.2	5	11.2	6
10.3	10	11.3	12
10.4	15		

TABLE 9. Parameters of Laser Shock Peening. Pulse frequency  $f = 30$  kHz, displacement  $s_x = s_y = 40$   $\mu$ m.

the thermal relaxation of macroscopic residual stresses after thermal annealing was also measured.

For air abrasive cutting overcoming of the yield stress was found out with increasing the pressure to 2.5 MPa. Due to rotational movement during air abrasive machining and water jet machining the values of surface residual stresses are isotropic.

Samples machined by laser exhibit thermal relax-

ation of residual stresses. At the same time, the found anisotropy of state of residual stresses is due to overlapping of laser-processed areas.

On the samples after the loading tests thermal relaxation of residual stresses was observed. It was shown that titancarbide is more sensitive to load than aluminium oxide. For more detailed information see [6].

#### ACKNOWLEDGEMENTS

This work was supported by grant Student Grant Competition CTU no. SGS16/246/OHK4/3T/14 and Grant Agency of the Czech Republic (no. 14-36566G).

Al <sub>2</sub> O <sub>3</sub>				TiC			
L direction RS MnK $\alpha$ (0210)				L direction RS CrK $\alpha$ (311)			
Sample	$\sigma_N$ [MPa]	$\sigma_S$ [MPa]	FWHM [2 $\Theta$ ]	Sample	$\sigma_N$ [MPa]	$\sigma_S$ [MPa]	FWHM [2 $\Theta$ ]
11.1	-42	27	0.693	11.1	-453	64	0.655
11.2	3	21	0.606	11.2	-129	76	0.530
11.3	-78	40	0.596	11.3	-242	49	0.577
T direction RS MnK $\alpha$ (0210)				T direction RS CrK $\alpha$ (311)			
Sample	$\sigma_N$ [MPa]	$\sigma_S$ [MPa]	FWHM [2 $\Theta$ ]	Sample	$\sigma_N$ [MPa]	$\sigma_S$ [MPa]	FWHM [2 $\Theta$ ]
11.1	-145	17	0.612	11.1	-348	95	0.580
11.2	-15	19	0.610	11.2	-190	59	0.563
11.3	47	24	0.649	11.3	-240	66	0.446

TABLE 11. The values of normal ( $\sigma_N$ ) and shear ( $\sigma_S$ ) residual stresses after stress testing.

## REFERENCES

- [1] R. Kumar, et al. Synthesis and characterization of al<sub>2</sub>o<sub>3</sub>+tic nano-composite by spark plasma sintering. *International Journal of Refractory Metals and Hard Materials* **577**:9–15, 2016.
- [2] Z. Yin, et al. Friction and wear behaviors of al<sub>2</sub>o<sub>3</sub>+tic micro-nano-composite ceramic sliding against metals and hard materials. *International Journal of Refractory Metals and Hard Materials* **577**:9–15, 2016.
- [3] A. Humár. *Materiály pro řezné nástroje*. First printing. MM publishing, 2008.
- [4] C. B. Carter, M. G. Norton. *Ceramic materials: science and engineering*. Second edition. Springer Science and Business Media, 2013.
- [5] M. University STANKIN. Materials for experimental measurement.
- [6] J. Němeček. Studium reálné struktury oxidových řezných keramik.